



Science Arts & Métiers (SAM)

is an open access repository that collects the work of Arts et Métiers Institute of Technology researchers and makes it freely available over the web where possible.

This is an author-deposited version published in: <https://sam.ensam.eu>
Handle ID: <http://hdl.handle.net/10985/7316>

To cite this version :

Kévin LE MERCIER, Michel WATREMEZ, Jean-Daniel GUERIN, Laurence FOUILLAND-PAILLE, Laurent DUBAR - Thermo-mechanical behaviour of spheroidal graphite iron in the austenitic phase - 2013

Any correspondence concerning this service should be sent to the repository

Administrator : scienceouverte@ensam.eu



Thermo-mechanical behaviour of spheroidal graphite iron in the austenitic phase

K. Le Mercier^{a,b,c}, M. Watremez^{a,b,c}, J.D. Guérin^{a,b,c}, L. Fouilland^{d,c} L. Dubar^{a,b,c}

a. Univ Lille Nord de France, F-59000 Lille, France

b. UVHC, TEMPO EA 4542, F-59313 Valenciennes, France

c. Institut Carnots Arts, F-75013 Paris, France

d. Arts et Métiers ParisTech, LMPF EA 4106, F-51006 Châlons en Champagne, France

Résumé :

L'objectif principal de cette étude est d'identifier le comportement thermomécanique de la fonte à graphite sphéroïdal (GS) EN-GJS-700-2 en phase austénitique. Des essais de traction et de compression sont réalisés sur un simulateur Gleeble 3500. Ce dernier permet de contrôler avec précision la température et la vitesse de déformation au cours des essais afin de déterminer leur influence sur le comportement mécanique de la fonte étudiée. La loi de comportement de Johnson-Cook de la fonte étudiée est obtenue par méthode numérique inverse. Enfin, des examens métallographiques sont réalisés par microscopie optique sur les éprouvettes post-mortem.

Abstract :

The main objective of this paper is to identify the thermo-mechanical behaviour at high temperature of the spheroidal graphite (SG) iron EN-GJS-700-2. In the first instance, tensile and compression tests in austenitic phase are performed. These experiments are carried out using Gleeble 3500 system enabling a precise control on testing temperature and strain rate. Indeed, the effects of these testing parameters on the SG iron behaviour are studied. Furthermore, a numerical inverse method is used to identify the Johnson-Cook constitutive model of this iron. Finally, post-mortem metallography of specimens is analyzed using optical microscopy.

Keywords : SG iron ; Thermo-mechanical behaviour ; Gleeble

1 Introduction

A few years ago, heat treated spheroidal graphite (SG) iron also called austempered ductile iron (ADI) emerged in several fields such as automotive or railway industries. This SG iron is obtained by an isothermal heat treatment called austempering. This consists in an austenitizing treatment in the temperature range between 850 and 950°C followed by quenching in the temperature range between 250 and 350°C where the pearlitic-ferritic matrix of SG iron transforms into ausferrite. Through this special heat treatment, ADI provides an efficient compromise between strength, fracture toughness and high resistance to abrasive wear at low cost. Therefore, ADI is intended to substitute forged steel for weight reduction of manufactured components.

To save time and energy so the manufacturing cost decreases, the use of a combined casting and forging process followed by the austempering treatment may be appropriate. The removal of risers and feeder head is thus performed at 1000°C just after the casting operation to be more competitive on production rate. However, this step may cause several surface degradations which jeopardize the process viability [1].

To evaluate sensitive parameters of the hot cutting operation, experiments on an orthogonal cutting test bench [2] are conducted on the EN-GJS-700-2 iron which can be heat treated to produce ADI. The objective is to understand the physical mechanisms responsible for the surface degradations.

Several tests are performed at 1000°C with different cutting speeds and the facies of cut surfaces are observed with optical microscope. This study highlights a brittle-ductile transition (BDT) occurring in the primary shear zone under spruing operation at low cutting speeds and high temperature (Fig.1).

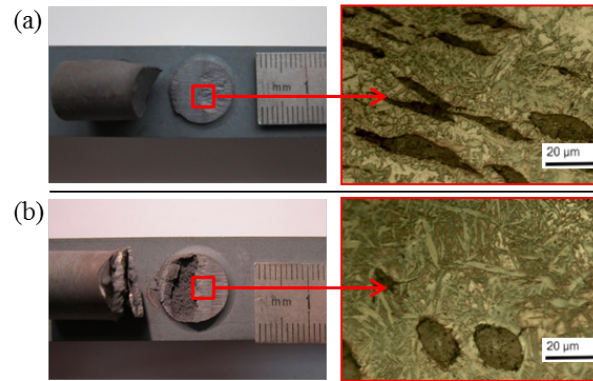


FIGURE 1 – Optical views of specimens cut face and microstructural details in a cross section for different cutting speeds. (a) 1.3 m.s⁻¹ ductile (b) 1.6 m.s⁻¹ brittle [1].

Indeed, for low cutting speed (Fig.1.a), a ductile fracture allows a spruing operation without surface degradation. Furthermore, the study of microstructural details in a cross section shows a grain refinement in comparison with a higher cutting speed. Therefore, the BDT is linked with the dynamic recrystallization (DRX) activation in the austenitic phase [1]. The present study deals with a local approach to explain the surface degradation phenomena during hot cutting process on SG iron. This consists in modelling the orthogonal cutting process with the Abaqus software but rheological behaviour of EN-GJS-700-2 iron has to be previously determined.

Therefore, this paper focuses on the mechanical behaviour of this SG iron at the austenitization temperature range (around 1000°C). Tensile and compression experiments are performed to seek for the presence of dynamic recrystallisation and to identify the Johnson-Cook constitutive model. Furthermore, metallography analysis of tested specimens allows to understand the microstructural mechanisms involved in the behaviour of the EN-GJS-700-2 iron.

2 Experimental procedures

The EN-GJS-700-2 iron specimens present at room temperature a pearlitic matrix and a small amount of ferrite surrounding the graphite nodules, called bulls eye ferrite (Fig.2). The chemical composition is given in Table 1.

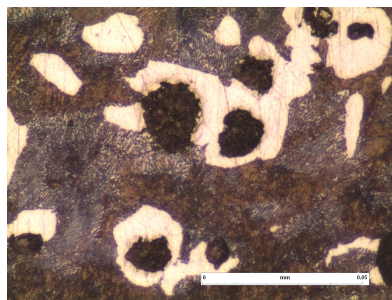


FIGURE 2 – Micrography of EN-GJS-700-2 etched with saturated picric acid (x50).

Element	C	Si	Mn	S	Cu	Ni	Cr	Mo	Mg
Composition (wt%)	3.35	2.72	0.16	0.009	0.87	0.71	<0.03	0.21	0.043

TABLE 1 – Chemical composition of EN-GJS-700-2 iron specimens.

The experiments are performed using a Gleeble 3500 thermo-mechanical simulator. This tensile-compression testing machine ensures a precise control of temperatures, loading and jaw speed during the test. Temperature is measured with K thermocouple located at the center of specimen. This device also allows to control the axial temperature gradient. The heating of specimens is carried out by resistive effect at $5^{\circ}\text{C}\cdot\text{s}^{-1}$ (Fig.3.b). The cooling rate is about $35^{\circ}\text{C}\cdot\text{s}^{-1}$ on tensile tests thanks to the use of cold jaws. Compression specimens are air cooled.

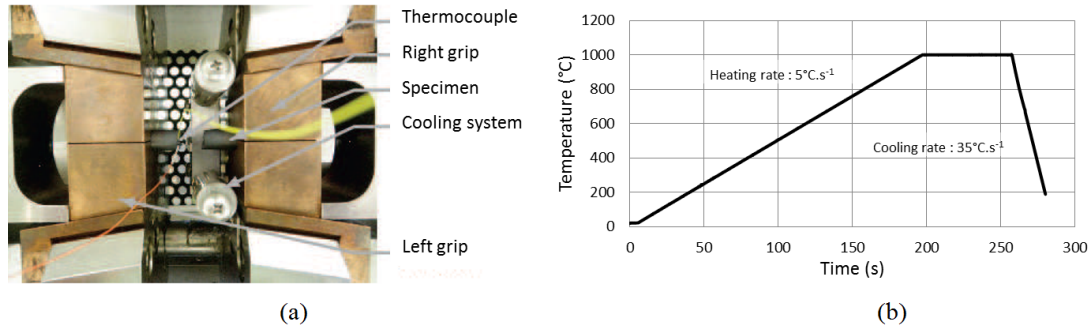


FIGURE 3 – (a) View of the Gleeble thermo-mechanical simulator. (b) Thermal sequence used during a test : heating from reference temperature to testing temperature, holding and finally cooling.

Tensile tests are performed at 800 and 1000°C for strain rates 1 and 10 s^{-1} . Compression tests are carried out at 1000°C for strain rates 0.5 and 1 s^{-1} . In order to consider dispersion of the results, at least two specimens are used for each testing parameter configurations. According to Fig.4 and Fig.5, the repeatability of tensile and compression tests is acceptable.

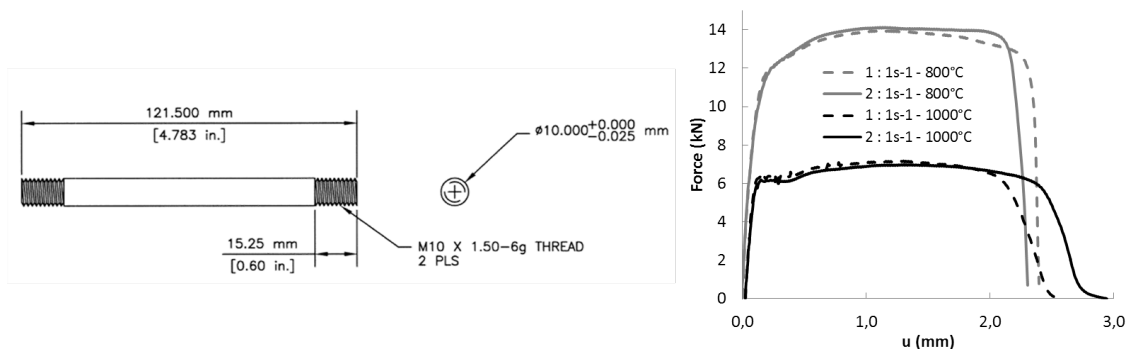


FIGURE 4 – Design drawing of 10 mm diameter tensile specimen and repeatability of tensile tests.

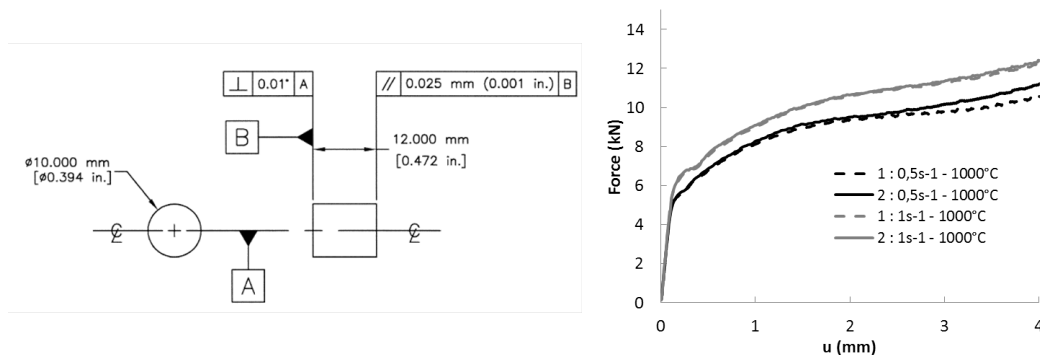


FIGURE 5 – Design drawing of 10 mm diameter compression specimen and repeatability of compression tests.

3 Results and discussion

3.1 Tensile tests

In order to get stress σ and strain ε , the following equations (1) are used. S_0 is the initial cross-section area of the specimen, l_0 is the initial length of the heated zone (10 mm). F and u are respectively the force and the displacement measured during the test.

$$\sigma = \frac{F}{S_0} \exp(\varepsilon) \quad ; \quad \varepsilon = \ln\left(1 + \frac{u}{l_0}\right) \quad (1)$$

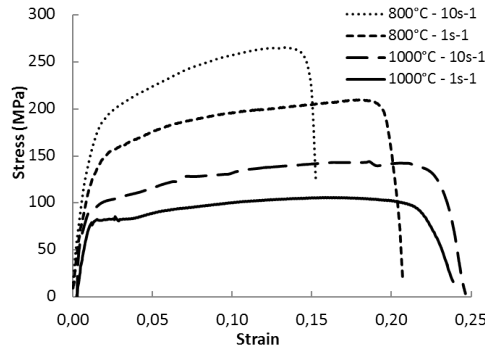


FIGURE 6 – Tensile stress-strain curves. Strain rates [1 - 10 s⁻¹] and temperatures [800 - 1000°C].

According to Fig.6, tensile experiments did not succeed to find evidences of dynamic recrystallization for these strain rate and temperature ranges.

The Johnson-Cook constitutive model is a five parameter empirical model that describes the yield stress σ as function of temperature, plastic strain and plastic strain rate. Equation (2) is the expression of this model where A , B are the strain-hardening coefficients, n is the strain-hardening exponent, $\dot{\varepsilon}_0$ is the reference strain rate, $\dot{\varepsilon}$ is the current strain rate, T_{melt} , T_{ref} and T are respectively the melting, the reference and the current temperatures and m is the temperature exponent.

$$\sigma = (A + B\varepsilon^n) \left(1 + C \ln\left(\frac{\dot{\varepsilon}}{\dot{\varepsilon}_0}\right)\right) \left(1 - \left(\frac{T - T_{ref}}{T_{melt} - T_{ref}}\right)^m\right) \quad (2)$$

The heated zone of tensile test is modelled with axisymmetric shell elements (CAX4T) in an Abaqus Standard simulation (Fig.7.a). The upper face of the specimen is controlled by velocity and lower face is locked. Thanks to an optimization process, called adaptative surface response method (ASRM), Johnson-Cook's model constants are identified.

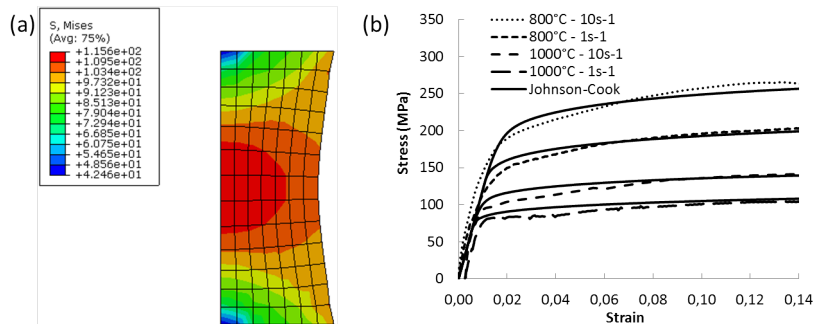


FIGURE 7 – (a) Abaqus simulation of tensile test. (b) Johnson-Cook fitting after optimization process.

Fig.7.b shows that Johnson-Cook constitutive model constants obtained by numerically inverse method are efficient. Therefore, the finite element simulation of tensile test is able to accurately predict the behaviour of EN-GJS-700-2 iron from 800°C to higher temperatures. However, fracture is not taken into account in this tensile test model and will be determined in further study. The coefficients resulting from the numerically inverse method are given in Table.2.

E (GPa)	A (MPa)	B (MPa)	n	C	$\dot{\epsilon}_0$ (s ⁻¹)	m	T_{ref} (K)	T_{melt} (K)
11.5	130	111.557	0.34	0.138	1	1.125	1073	1473

TABLE 2 – Young's modulus and identified Johnson-Cook constitutive model constants for EN-GJS-700-2 iron at high temperature.

3.2 Compression tests

To determine stress-strain curves, an analytical method [3] based on the following equations is used. F is the current upsetting load, R is the mean current radius of the specimen, Z is the barrelling coefficient (Equation (5)), H_i and H are respectively the initial and current heights of the specimen, α is the upsetting ratio and m_f is the mean sub-layer friction factor. This friction factor is determined from the barrelling and height ratios of the tested specimen, here it is set to 0.7.

$$\sigma = \frac{F}{\pi R^2 Z} \quad ; \quad \varepsilon = \ln\left(\frac{H_i}{H}\right) \quad (3)$$

$$R = R_i \sqrt{\frac{H_i}{H}} \quad ; \quad \alpha = \frac{H}{R} \quad (4)$$

$$Z = \frac{8b}{\alpha} \left\{ \left[\frac{1}{12} + \left(\frac{\alpha}{b}\right)^2 \right]^{\frac{3}{2}} - \left(\frac{\alpha}{b}\right)^3 + \frac{m_f}{24\sqrt{3}(e^{b/2}-1)} \right\} \quad ; \quad b = \frac{4m_f\alpha}{\sqrt{3}} \left(1 + \frac{2m_f\alpha}{3\sqrt{3}}\right)^{-1} \quad (5)$$

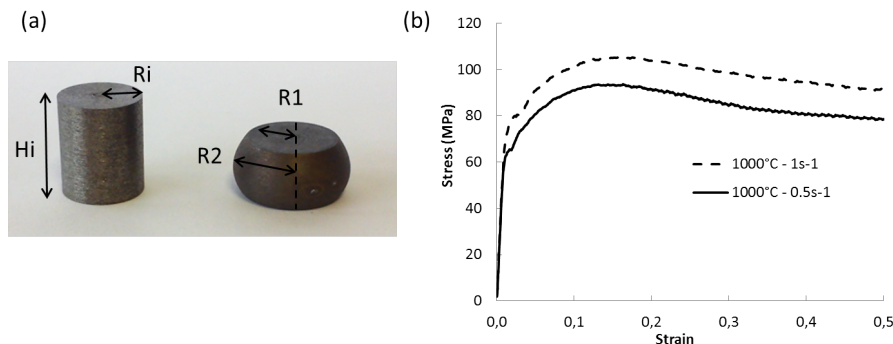


FIGURE 8 – (a) Picture of the initial and final shape of the compression specimen. (b) Gleeble compression stress-strain curves : Strain rates [0.5 - 1 s⁻¹] at 1000°C.

Fig.8.b curves shows a peak in the flow stress followed by a stabilization which is specific to dynamic recrystallization [4]. Furthermore, this recovery phenomenon is approximately the same for both strain rates. The metallography analysis of tested specimens is necessary to corroborate or invalidate these observations.

3.3 Symmetric behaviour and metallography analysis

The EN-GJS-700-2 presents at 1000°C a symmetric tensile-compression behaviour as shown in Fig.9.a. Furthermore, dynamic recrystallization occurring during compression test seems to be a large strain phenomenon. Post-mortem metallography of both specimens presents a martensitic matrix and spheroidal graphite. Compression specimens (Fig.9.c) show finer martensite needles than tensile specimen (Fig.9.b). This is an indicator of the dynamic recrystallization activation [1].

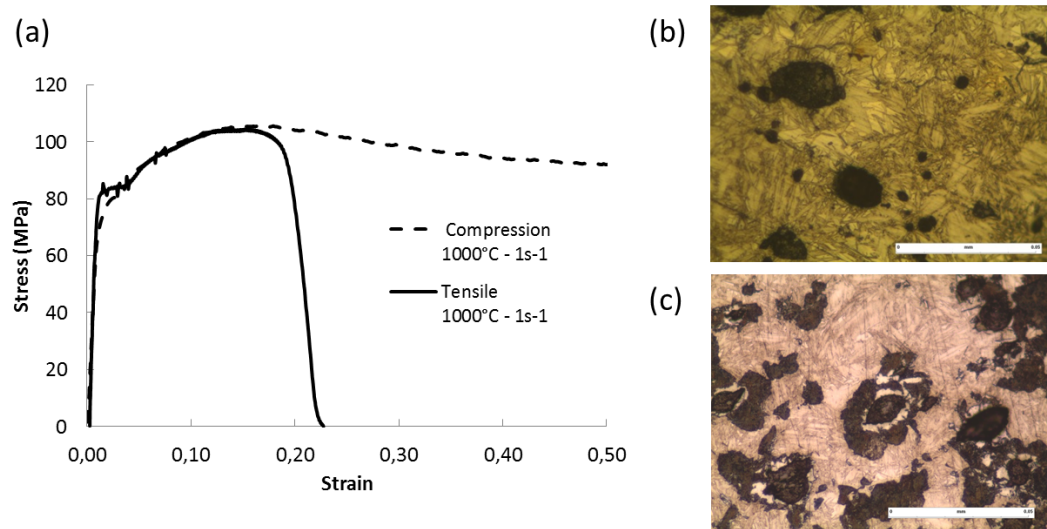


FIGURE 9 – (a) Absolute value of tensile and compression stress-strain curves [1000°C and 1s^{-1}]. Post-mortem metallography (x50) of corresponding tensile (b) and compression (c) specimens, etched with saturated picric acid.

4 Conclusion

The experiments performed in this study highlight the symmetric tensile-compression behaviour of the EN-GJS-700-2 iron in its austenitic phase. Further tests have to be performed to confirm or invalidate this at lower temperatures.

Dynamic recrystallization did not appear during tensile experiments. However, this iron seems to be subjected to dynamic recrystallization (DRX) under compression tests. This confirms the observations performed on the orthogonal cutting test bench. Moreover, upcoming compression tests will aim to find the dynamic recrystallization activation range and metallographic examinations of compression specimens will be more detailed.

The Johnson Cook constitutive model of EN-GJS-700-2 is now available for high temperatures. Nevertheless, dynamic recrystallization is not implemented in this rheological law.

In high speed machining, strain rates are very high [5]. Therefore, shear tests on specific hat-shaped specimens often used to identify rheological law for these strain rates [6] are envisaged.

Finally, modelling the dynamic recrystallization during the orthogonal cutting process is also envisaged. This will be useful to predict the emergence of surface degradations.

References

- [1] Fouillard, L., El Mansori, M. 2012. Experimental study of the brittle-ductile transition in hot cutting of SG iron specimens. *Journal of Materials Processing Technology*. **213** 201-213
- [2] Grzesik, W. 2008. Orthogonal and Oblique Cutting Mechanics. *Advanced Machining Processes of Metallic Materials*. 69-84
- [3] Guérin, J.D., Oudin, J., Bricout, J.P. 1995. Analytical and finite-element analysis of in-situ solidified specimen upsetting. *Journal of Materials Processing Technology*. **49** 399-423
- [4] Mirzadeh, H., Najafzadeh, A. 2010. Prediction of the critical conditions for initiation of dynamic recrystallization. *Materials and Design*. **31** 1174-1179
- [5] Watremez, M., Meresse, D., Dubar, L. Brocail, J. 2012. Finite element modelling of orthogonal cutting : sensitivity analysis of material and contact parameters. *International Journal of Simulation and Process Modelling*. **7** 262-274
- [6] Hor, A., Morel, F., Lebrun, J.L., Germain, G. 2013. An experimental investigation of the behaviour of steels over large temperature and strain rate ranges. *International Journal of Mechanical Sciences*. **67** 108-122